Recommended Practice Guide for Carbon Nanotube Characterization

Chapter 3. Near-Infrared (NIR) Spectroscopy

Mikhail E. Itkis and Robert C. Haddon

Center for Nanoscale Science and Engineering,

Departments of Chemistry and Chemical & Environmental Engineering

University of California, Riverside, CA 92521-0403

3. Near-Infrared (NIR) Spectroscopy

3.1 Introduction

Near-IR (NIR) spectroscopy is an analytical technique which is ideally suited for the characterization of single-walled carbon nanotubes (SWNTs), because it allows the measurement of the absorption of light in the region of the interband electronic transitions. These electronic transitions are the characteristic signature of the SWNT electronic structure and may be observed in the solution or solid state as a function of photon energy. NIR transmission spectroscopy has been extensively used to detect SWNT interband transitions,[1-8] to evaluate the effect of ionic and covalent chemistry on the band structure, [7, 9-13] and to compare the abundance and diameter distribution of the SWNTs produced by different synthetic techniques as a function of synthetic parameters and catalyst composition.[14-17]

Recently, NIR spectroscopy has been advanced as an efficient tool to quantitatively evaluate the carbonaceous purity of bulk SWNT material.[18-22] The procedure is extremely simple, can be efficiently used by students and technical personnel and utilizes equipment that is routinely available in many research and educational laboratories. In this chapter we formulate the main principles of the NIR spectroscopy-based purity evaluation technique. We present examples of the practical use of this technique for optimization of SWNT synthesis and for improving the parameters of a purification procedure. We provide an assessment of the advantages and potential limitations of this purity evaluation technique against other carbon nanotube purity assessment methods.

3.2. Formulation of method: Electronic Structure and Optical Spectroscopy of SWNTs

The electronic structure of SWNT derives from that of a 2-D graphene sheet, but because of the radial confinement of the wave function the continuous electronic density of states (DOS) in graphite divides into a series of spikes in SWNTs which are referred

to as Van Hove singularities (Figure 1).[23-26] Depending on helicity and diameter, these 1-D nanostructures may be metals or semiconductors.[23-26]

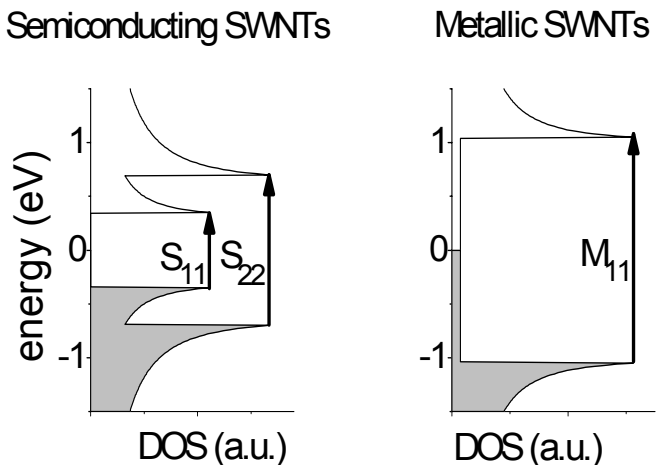

Figure 1: *Electronic density of states (DOS) of semiconducting and metallic SWNTs*

Based on simple tight-binding theory, the semiconducting SWNTs give rise to a series of electronic transitions between the principal mirror spikes in the electronic density of states (DOS) starting with $S_{11} = 2a\beta/d$ and $S_{22} = 4a\beta/d$, while the metallic SWNTs show their first transition at $M_{11} = 6a\beta/d$, where a is carbon-carbon bond length (nm), β is the transfer integral between $p\pi$-orbitals (β = ~2.9 eV) and d is SWNT diameter(nm).[5, 23-26] Current synthetic techniques produce SWNTs with a range of chiralities and diameters, and in this case the S_{11}, S_{22} and M_{11} features are simultaneously present in the electronic spectra of the bulk SWNT sample with individual features broadened due to the finite SWNT diameter distribution.[2, 3, 5, 7, 8] NIR optical absorption spectroscopy can capture these specific features which typically occur between 0.5 and 3 eV.[2, 3, 5, 7, 8] The optical spectra of carbonaceous and graphitic impurities present in bulk SWNT samples give rise to a featureless monotonically increasing absorption in this spectral region (0.5 – 4 eV).[18-20, 27, 28] These spectral characteristics provide a unique opportunity to distinguish between the SWNTs and impurities present in the sample using optical spectroscopy.

Figure 2 shows a schematic of the absorption spectrum of a typical electric arc discharge (EA) produced SWNT sample in the spectral range between the far-IR and the UV (10 - 45 000 cm^{-1}), with the absorptions due to SWNTs and carbonaceous impurities shown in different colors to illustrate the different components (although it is not yet possible to analytically separate these contributions).[19, 20] The high-energy part of the spectrum is dominated by the π-plasmon absorption from both SWNTs and carbonaceous impurities, and the tail of this peak extends into the far-IR part of the spectrum. The NIR - visible part of the spectrum from 4000-17 000 cm^{-1} exhibits characteristic absorption features, originating from the interband transitions between pairs of Van Hove singularities in semiconducting and metallic SWNTs, which ride on the top of the π-plasmon tail. It is intuitively understandable, that the strength of these characteristic features in comparison with the featureless baseline provides a measure of the purity of the SWNT material.

While the S_{11} transition is the most prominent, we chose the second semiconducting transition (S_{22}, inset to Figure 3), for the purity evaluation because the S_{22} transition is less susceptible to incidental doping and because it matches the transmission window for dimethylformamide (DMF) which is utilized for the solution (dispersion) phase NIR

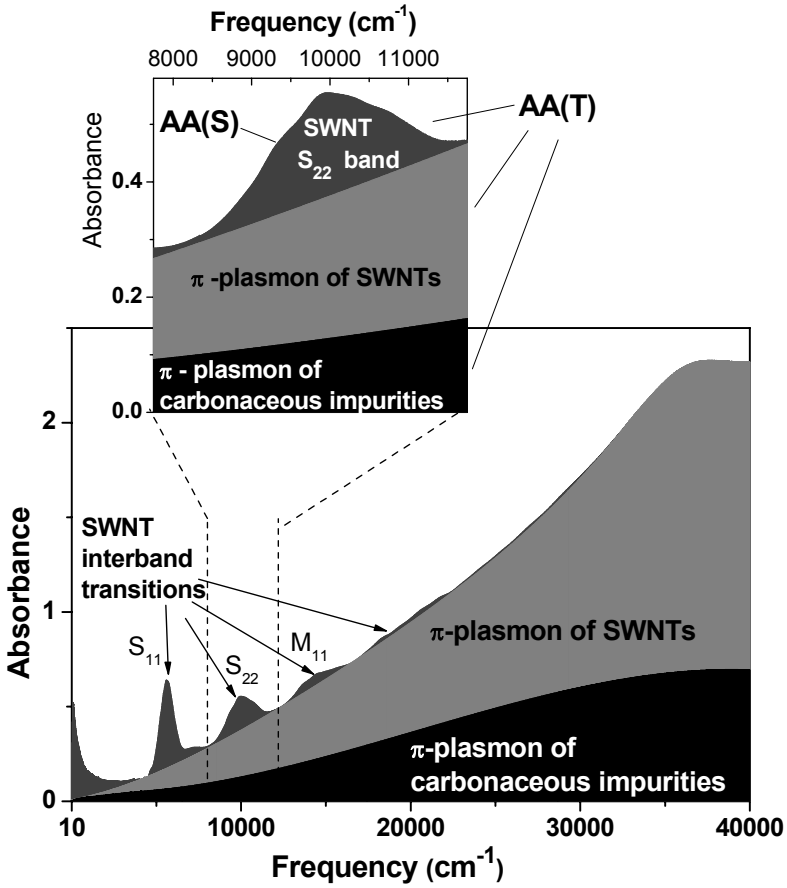

Figure 2: Schematic illustration of the optical spectrum of typical SWNT sample produced by the electric arc method. Inset shows the region of the S_{22} interband transition utilized for NIR purity evaluation. In the diagram: AA(S) is the area of S_{22} spectral band after linear baseline correction; AA(T) is the total area of the S_{22} band including SWNT and carbonaceous impurity contributions. The NIR relative purity is given by RP = (AA(S)/AA(T))/0.141 (see text).

spectroscopy.[18-20] It is known, that DMF is one of the most efficient solvents for dispersing both raw and purified SWNT material, and we have found that DMF can partially compensate the incidental doping affecting the S_{22} interband transition.[18-20]

We have identified the ratio AA(S)/AA(T) as the simplest possible metric of SWNT purity,

where AA(S) is the area of the S_{22} interband transition after linear baseline subtraction (dark gray area in the inset to Figure 2), and AA(T) is the total area under the spectral curve, with both areas taken between the spectral cutoffs of 7750 and 11750 cm^{-1}, which were chosen to capture the S_{22} interband electronic transitions of SWNTs of the diameter produced by the EA-process with Ni/Y catalysts.[18-20] This ratio is then normalized by dividing by 0.141, the value of AA(S)/AA(T) obtained for an arbitrary high purity reference sample of AP-SWNTs (denoted R2), and this procedure therefore gives rise to a relative purity (RP).[18-20] Because a 100% pure reference sample is not currently available, it is not possible to give an absolute determination of SWNT purity, although progress may be noted.[27, 28] Nevertheless, through the joint efforts of the carbon nanotube community, and with sample exchanges between research groups it will be possible to further refine the choice of a reference sample and to asymptotically converge on a standard for the measurement of absolute purity.

3.3 Practical Procedure

3.3.1 Choice of Spectrophotometer

Common FT-IR spectrometers cover the spectral range between 10 000 and 400 cm^{-1} (1000 – 25 000 nm), whereas UV-Vis spectrophotometers usually cover the range between 175 and 900 nm (57 000 – 11 000 cm^{-1}). In order to cover the typical S_{22} and M_{11} interband transitions which are of interest in the purity evaluation of SWNTs produced by electric arc and laser ablation techniques, a spectral range of 7000-19 000 cm^{-1} is required, so neither of these types of spectrophotometers encompass the required spectral range. Several commercial instruments combine the UV-Visible and NIR spectral ranges and are suitable for the NIR purity evaluation procedure, including the Cary 500(5000) spectrophotometer and equivalent instruments from Shimadzu and Perkin-Elmer with spectral range 57 000 – 3000 cm^{-1} (175 – 3300 nm).

3.3.2 Sample preparation

For accurate evaluation of bulk quantities of SWNT material (>10g), special attention must be paid to the preparation of the NIR samples, because as-prepared SWNT (AP-SWNT) material is typically very inhomogeneous. Below we present a multi-step best

practices procedure developed for large scale batches of inhomogeneous AP-SWNT material:[18-20]

Step 1. The AP-SWNT material is mechanically homogenized to give a dry powder. The use of a kitchen blender operated at low speed for 5 min leads to a fine homogeneous powder.

Step 2. Homogenized AP-SWNT soot (50mg) is dispersed in 100 ml of DMF by use of an Aquasonic 50T, 75T, or 550T ultrasonic bath or equivalent brand for 10-20 min. Mechanical stirring facilitates homogenization during this step which should lead to a homogeneous concentated slury of SWNTs in DMF.

Step 3. A few drops of the concentrated SWNT slurry is collected by pipette from different regions of the sample and diluted to 10 ml with fresh DMF and sonicated for 10 minutes. By use of one or two additional 10 ml scale dilution-ultrasonication cycles the concentration is reduced to ~0.01 mg/ml, which provides a stable, visually non-scattering dispersion with an optical density close to 0.2 at 12,000 cm^{-1} in a 10 mm path-length cell.

This preparation procedure results in a test sample, which provides a reproducible and accurate representation of the carbonaceous purity of bulk AP-SWNT soot. Increasing the SWNT concentration in the final test sample improves the signal-to-noise ratio of the experimental optical spectrum, but may destabilize the dispersion and lead to significant light scattering and thereby compromise the results of the purity evaluation.

For purified SWNT samples the amount of material utilized for the purity evaluation test can be reduced to a few mg because the material is usually fairly well homogenized and less material is required to give a statistically representative sample. In order to assure homogenization we recommend the use of a standard coffee blender to convert purified SWNT material into a fine powder.

3.3.3 Practical example of spectral measurements and relative purity calculations

The SWNT sample should be ultrasonicated just before the spectral measurement in order to assure high quality dispersion, and the spectrometer should be turned on 30 minutes prior to the measurement to allow the baseline to stabilize. Spectra are usually taken in the range 7000-17 000 cm^{-1} for EA-produced SWNTs in order to visualize both the S_{22} and M_{11} interband transitions. Some spectrophotometers allow the collection of spectra only as a function of wavelength. For purity calculations we recommend processing the data as a function of frequency (energy) as shown in Figure 3, because the absorbance spectra as a function of wavelength (proportional to inverse energy) show significantly more curvature and are more difficult to analyze.

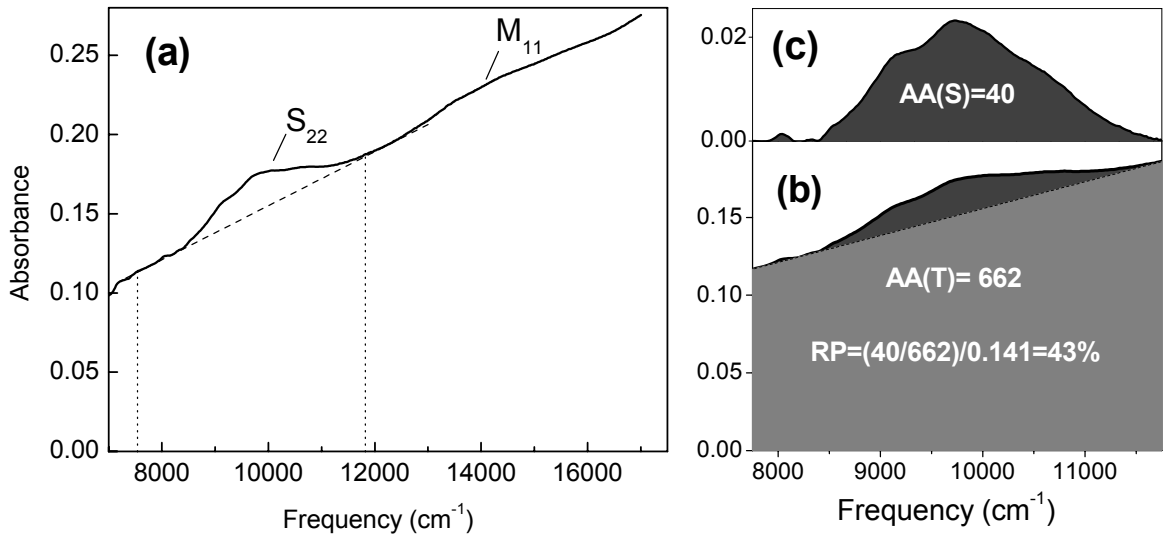

Figure 3: *Practical procedure for determination of relative purity (RP) of AP-SWNT sample: a)Solid line: spectrum of SWNT dispersion in DMF in the range 7000-17 000 cm^{-1}, dashed line: linear baseline, dotted lines: spectral cutoffs for purity determination; b) Total area AA(T) (black + gray) in the region of the S_{22} interband transition, calculated integral AA(T)=662; c) Area of S_{22} feature AA(S)(gray) after linear baseline correction, integral AA(S)=40. RP = 43%*

In order to establish the baseline a tangent line is drawn to the minima of the absorption curve at the low and high energy sides of the S_{22} transition (Figure 3a); in practice it is best to use 5 data-points on each side of the chosen S_{22} spectral window (7750 – 11750 cm^{-1} for EA -SWNTs) for the linear fitting routine. The absorption spectrum within the cutoffs is presented separately in Figure 3b with calculated total area AA(T) = 662. Figure 3c shows the spectrum of the S_{22} feature after linear baseline correction with integrated area AA(S)=40. The ratio AA(S)/AA(T) is divided by 0.141 to obtain a relative purity, RP against the P2 reference sample:[18-20] in the present case RP = 43% (Figure 3).

3.3.4 Most common source of experimental errors: distorted baseline

Figure 4 presents a NIR spectrum of a SWNT dispersion in DMF exhibiting both of the two most common spectral distortions which occur in the vicinity of 8000 and 12 000 cm^{-1} (red arrows). The distortion just above 8000 cm^{-1} is due to presence of traces of water in the solvent which gives very strong absorptions that in some cases can not be properly subtracted from the baseline by the pure solvent in the reference channel.

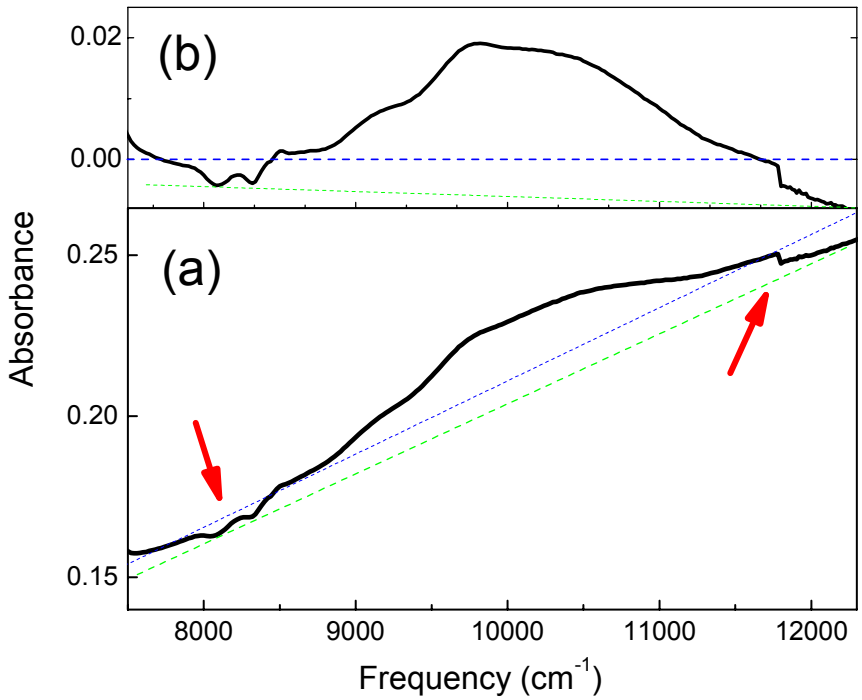

Figure 4: *Example of distortions in NIR spectra (red arrows) due to the presence of traces of water in the DMF and the change of optical elements in the spectrophotometer. (a) complete spectrum, (b)spectrum of S_{22} feature after linear baseline correction. Choice of baseline is uncertain (between blue and green dashed lines), which leads to uncertainties in the integrated areas AA(T) and AA(S) and in the calculated value of the relative purity.*

In the example given in Figure 4 this distortion produces a negative contribution to the integrated area thus reducing the relative purity because of the uncertainty in the baseline position at the low energy spectral cutoff. It is important to use dry solvent and to avoid admitting any traces of water to the solvent during the sample preparation procedure.

The step in the trace in the vicinity of 12 000 cm^{-1} corresponds to the change from the NIR detector to the UV-Vis detector in the spectrophotometer and introduces errors into

spectrum and the linear baseline correction near the high-energy spectral cutoff. Possible baseline choices are shown by green and blue colors and this uncertainty serves to introduce errors into the calculated RP. The jumps in the spectrum result from the change of the optical elements inside the spectrophotometer and can be minimized by careful alignment of spectrophotometer components by the manufacturer, optimum alignment of the sample positions in both optical channels, by modifying the ratio of spectral resolutions in the NIR and UV-Vis spectral ranges, and by stabilization of the spectrometer by utilizing an extended warm-up time. It is practically impossible to avoid such steps in the case of scattering samples such as poorly dispersed SWNTs or inhomogeneous or thick SWNT films.

3.4 Characterization of NIR method

3.4.1 Reproducibility of the purity evaluation

To test the reliability of the NIR technique and the reproducibility of the purity measurements we prepared five independent 50 mg probe samples from the same mechanically homogenized 10g batch of AP-SWNT material using the recommended procedure.[18-20] The results of the NIR relative purity measurements are presented in the Figure 5. The five probe samples show an average relative purity of 46% with a standard deviation, SD = 3.0%, which corresponds to relative error ~7% in the measured RP value.

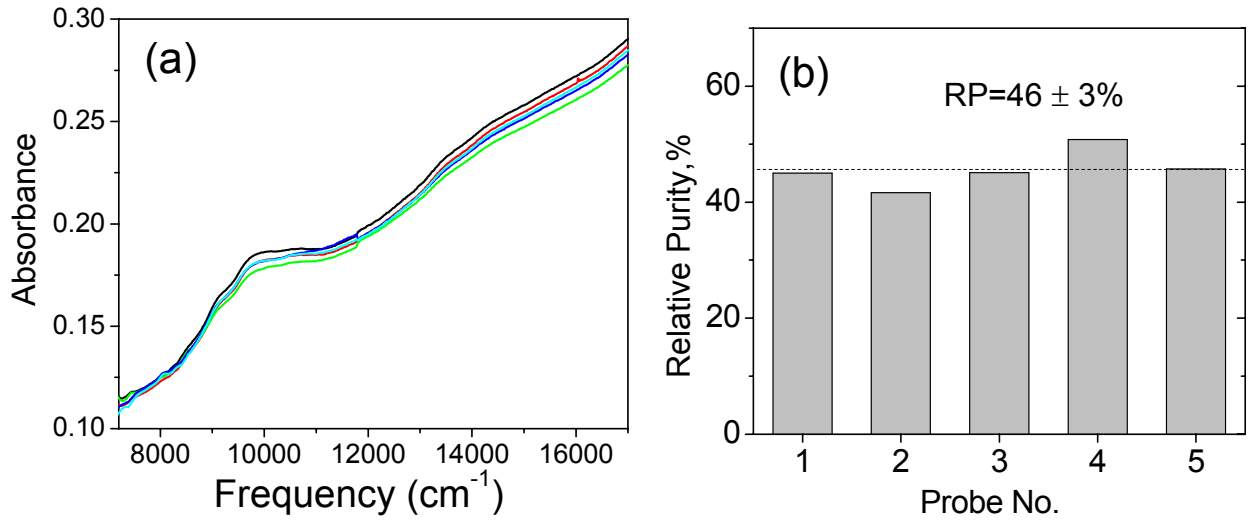

Figure 5: *Reproducibility test of NIR purity evaluation technique: a) Solution phase NIR spectra of five independent probe samples obtained from 10g AP-SWNT sample; b) Calculated purity of the five probe samples*

3.4.2 Influence of light scattering

The NIR purity evaluation method depends on the absorption of light, but the interaction of electromagnetic radiation with SWNTs may lead to scattering.[19, 20, 29] The occurrence of light scattering would be a complicating factor in the interpretation of the absorption spectra of SWNTs and might affect the accuracy of the purity evaluation by contributing to the level of the baseline (Figure 3), thus reducing the measured purity. The spectral contribution to light scattering (S) is controlled by the ratio of the characteristic dimension of the scattering particles (*d*) and the wavelength of the incident light (λ). In the present situation, we consider the SWNT length to be the characteristic dimension *d*, because the strongest interaction of light with SWNTs occurs when the light is polarized along the SWNT axis. Most SWNT samples show a wide length distribution, which is typically concentrated in the range d = 0.5 - 3 μm and this is comparable with the wavelength of light in vicinity of the S_{22} interband transition ($\lambda \approx$ 1 μm) that is utilized for purity evaluation. In this circumstance ($d \sim \lambda$) Mie scattering is expected to dominate,[19] and this scattering mechanism becomes more important as the particle size increases

($d > \lambda$) In the spectral range of interest there is a crossover between $\lambda > d$ and $\lambda < d$, and this makes it difficult to theoretically estimate the influence of scattering on the NIR absorption spectra, especially in the case of SWNT solution samples which present themselves to the light beam as dynamic highly anisotropic particles.

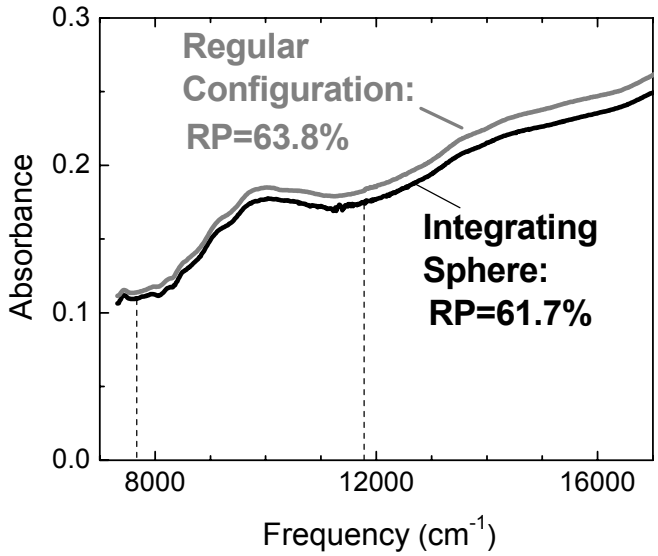

Figure 6: *Solution phase absorption spectra of a SWNT sample collected with the spectrophotometer in regular transmission configuration (gray curve) and using an integrating sphere (black curve) to collect the scattered light.*

In order to experimentally address these questions, we made use of an integrating sphere in the sample compartment of the Cary 500 UV-Vis-NIR spectrophotometer utilized in our experiments,[20] as discussed previously.[29] The integrating sphere recovers a significant fraction of the scattered light normally lost with the narrow aperture of collection presented in a standard transmission experiment. Figure 6 shows the NIR absorption spectra of an AP-SWNT dispersion in DMF measured with regular and integrating sphere configurations for the collection of light.[20] The introduction of the integrating sphere collection leads to a small decrease in the level of the baseline, and the calculated relative purities were found to be RP = 63.8% in regular, and RP = 61.7% in the integrating sphere configurations; Table 1 shows a comparison for three AP-SWNT samples with relative purities between 20 and 60%.[20] If scattering were to

be significant, we would expect a reduction in the relative purity, when measured in the regular configuration in comparison with the case of the integrating sphere technique. Table 1 shows the opposite trend, with a lower measured relative purity in the integrating sphere configuration, although the deviations are within the experimental accuracy of our

Table 1. Measured NIR Purity with Spectrophotometer in Regular and Integrating Sphere Configuration

Sample Number	1	2	3
Regular Configuration	20.5%	38.5%	63.8%
Integrating Sphere	16.5%	35.5%	61.7%

technique.[18-20] This suggests, that in the case of properly dispersed SWNTs, scattering does not materially affect the NIR relative purity evaluation. Incompletely dispersed samples with large aggregates of SWNTs would be expected to affect the purity evaluation as a result of Mie scattering, and it was for this reason that we emphasized the importance of the sample preparation procedure and stressed the necessity of utilizing low SWNT solution concentrations ($\leq$ 0.01 mg/ml).[18-20] It proved to be more difficult to control scattering in the case of SWNT thin films, and this was one factor which lead to our choice of solution phase.[18-22] rather than thin film[7, 14, 15, 17] transmission spectroscopy for the relative purity evaluation studies.

3.4.3 Influence SWNT concentration on relative purity determination

We previously recommended a concentration of 0.01 mg/mL for the SWNT purity evaluation;[18] higher SWNT concentrations are difficult to stabilize as non-scattering dispersions, while reducing the concentration decreases the signal to noise ratio of the

NIR spectra. In order to evaluate the importance of the SWNT concentration for NIR spectroscopy-based purity evaluation technique we prepared a series of dispersions of AP-SWNTs with concentrations between 0.05 and 0.001 mg/mL.[20] Figure 7 shows the NIR relative purities obtained from the NIR spectra shown in the inset, as a function of SWNT concentration.

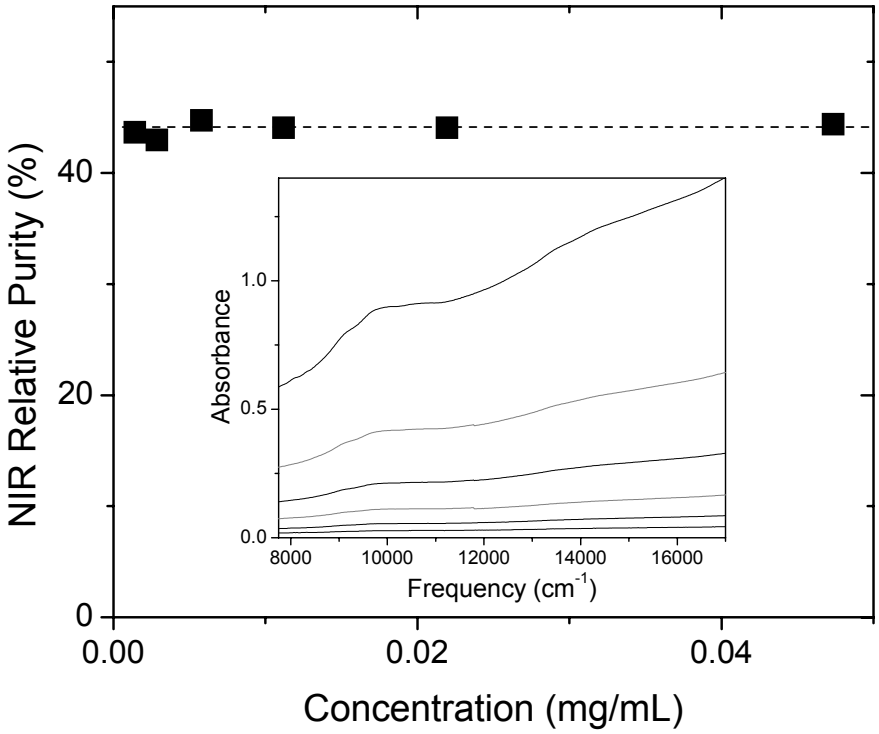

Figure 7: *NIR relative purity as a function of the concentration of the SWNT dispersion; inset shows experimental NIR solution phase spectra utilized for calculation of purity.*

Figure 7 demonstrates that the NIR relative purity values are independent of the SWNT concentrations, which is a simple consequence of the applicability of Beers law to SWNT dispersions.[27, 28] This confirms that the relative purities determined by the NIR technique are internally consistent, and that the sample preparation procedure does not require exact matching of the concentrations.

3.5 Examples of the application of NIR purity evaluation procedure

3.5.1 Optimization of SWNT synthesis

Figure 8 illustrates the use of the NIR-based purity evaluation technique for the study of the effect of the Y concentration on the large scale Ni/Y catalyzed EA-discharge Ni/Y production of SWNTs.[16] The bottom panels in Figure 8(a-e) show the region of the solution phase NIR spectra in the range of 7750-11750 cm^{-1} corresponding to the S_{22} interband transition for five Y concentrations between 0.25 and 8 atom% .

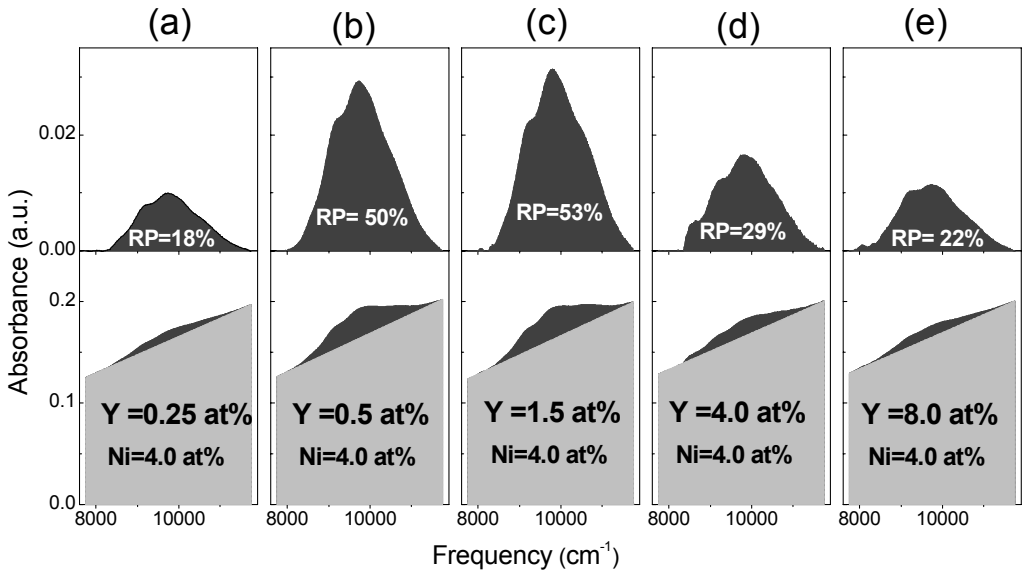

Figure 8: *Solution phase NIR spectra of EA-AP-SWNT soot produced with Ni-Y binary catalyst as a function of the Y concentration at a constant Ni concentration of 4 atom %. Bottom panel: spectra in the range of S_{22} interband transition consisting of featureless background (gray area) and S_{22} SWNT feature (black area) separated by the linear baseline; Top panel: the enlarged S_{22} interband transition obtained after the linear baseline subtraction. The relative carbonaceous purity of the AP-SWNT soot (top panel), is determined from the ratio of the area under the spectral curve in the top panel to the total spectral area in the bottom panel.*

The top panels in Figures 8(a-e) show the corresponding S_{22} features extracted from the original spectra (bottom panel) by a linear baseline correction. High purity SWNT samples have a high ratio of the area of the S_{22} band (top panel) to the total area under the spectral curve (bottom panel). It is clear from Figure 8 that the highest ratio and therefore the highest purity occurs in the vicinity of Y concentrations of 0.5 and 1.5 atom% in agreement with prior work.[30] Thus, the NIR technique provides an efficient tool to visualize and analytically evaluate the effect of catalyst composition and other synthetic parameters on the purity of the AP-SWNT product.[16, 21]

3.5.2 Evaluation of efficiency of purification and optimization of purification parameters

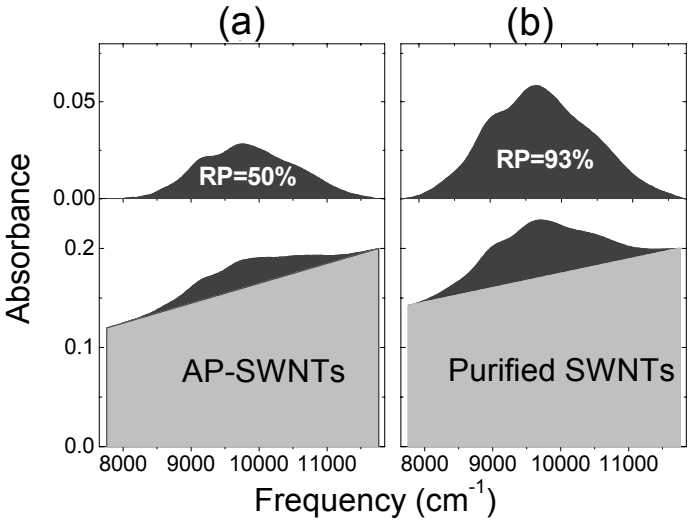

Figure 9: *NIR evalution of efficiency of purification procedure. NIR spectra in the range of the SWNT S_{22} interband transition for: (a) starting (AP) sample (NIR RP=50%), (b) purified (NIR RP=93%) sample; bottom panel – full spectra, top panel - S_{22} band after linear baseline subtraction.*

An important application of a purity evaluation technique is the ability to efficiently monitor and optimize the parameters of purification processes.[31-33] Figure 9 shows the NIR spectra of starting AP-SWNT material and the final purified product obtained by

oxidation of AP-SWNTs in air followed by treatment with hydrochloric acid. According to the NIR evaluation procedure the carbonaceous relative purity increased from 50 to 93% as a result of the purification (Figure 9) and the amount of residual metal catalyst decreased from 30 to 8%, as determined by TGA.

It is convenient to introduce the purification recovery factor PRF,[31, 33] which takes into account both the increase of purity and the loss of product; for an ideal process the product is analytically pure and PRF = 1.[33] If Y is the yield of the process then we have shown that the PRF is given by:[33] PRF = [RP(P-SWNT)/RP(AP-SWNT)] $\times$ Y, where RP(P-SWNT) and RP(AP-SWNT) are the relative purities of the as-prepared and purified SWNTs. Because the NIR technique applies to the carbonaceous purity of the sample the measured yield must be corrected for changes in the metal content of the sample and in this case the yield is given by $Y = [M_{fin} \times (1-MET_{fin})]/[M_{st} \times (1-MET_{st})]$, where M_{st} (M_{fin}) and MET_{st} (MET_{fin}) are the sample mass and the fraction of metal, respectively, in the starting material (final product). For example, in the purification procedure of AP-SWNTs illustrated in Figure 9, M_{st} =10g, RP(AP-SWNT) =50% and MET_{st} = 0.3 (metal residue of 30% determined by TGA); after purification M_{fin} = 2.5g, RP(P-SWNT) = 93% and MET_{fin} =0.92; leading to PRF = 0.61 for the process. Thus about 40% of the SWNTs present in the starting sample were lost during the purification process. Each step of a purification procedure can be evaluated and optimized on the basis of NIR relative purity and PRF figure of merit,[31-33] taking into account that the ideal purification process results in a PRF = 1.

3.6 Frequently asked questions about the capabilities and limitations of the NIR technique:

3.6.1 The NIR technique provides a value for the relative purity (RP) - what about the absolute purity?

At the present moment it is not possible to provide an absolute value of the purity of SWNTs, but it is expected that the widespread adoption of the NIR purity evaluation technique supported by other analytical techniques presented in this guide will soon produce samples which cannot be further purified and may thus be considered

analytically pure. The joint efforts of the carbon nanotube community, and sample exchanges between research groups will be required to asymptotically converge on a standard for the measurement of absolute purity. Based on currently available samples, we expect analytically pure SWNT samples to be characterized by values of AA(S)/AA(T) ~ 0.325, and RP ~ 230% when evaluated against the original reference sample R2.[20, 28]

3.6.2 To which types of SWNTs is the NIR purity evaluation technique applicable?

The NIR purity evaluation technique was initially developed for electric arc produced SWNTs prepared with the Ni/Y catalyst, but it has been already successfully adapted to SWNTs produced by laser ablation.[34] For the applicability of NIR technique it is important that the SWNTs have a relatively narrow diameter distribution without overlap between the S_{11}, S_{22} and M_{11} bands.[28]

3.6.3 Is the NIR technique applicable to CVD produced SWNTs?

The chemical vapor deposition (CVD) technique usually produces SWNTs with an extremely wide diameter distribution. As a result, there is significant overlap of the interband transitions in these preparations and this obscures the NIR spectral features and severely complicates the application of the current procedure. Recently, much higher selectivity of SWNT diameters and chiralities was achieved by modifying the catalyst preparations used in the CVD technique,[35] and by the application of separation procedures,[36] and the technique is applicable to such samples.

3.6.4 Is NIR technique applicable to HiPco produced SWNT?

The SWNT diameter distribution of HiPco SWNTs is wider than that of SWNTs produced by the electric arc and laser ablation techniques, but narrower than that of most CVD-produced SWNTs. In the optical spectra of HiPco material S_{11}, S_{22} and M_{11} bands are partially overlapping, so the direct calculation of AA(S)/AA(T) ratio results in an underestimated relative purity. Nevertheless, the utilization of the NIR technique can be very useful for the comparison of SWNT content from batch-to-batch for both manufacturers and end-users of HiPco SWNTs, so an internal HiPco reference

standard should be developed. Currently, there is no algorithm available to compare the purity of the best laser produced material against the best HiPco produced sample, so the development of absolute purity standards for each production technique is very important.[28]

3.6.5 Why is the linear baseline approximation used in the NIR purity evaluation procedure when a non-linear baseline fit might be more accurate?

We utilized the linear baseline approximation, because it provides a simple, easily applicable and consistent purity evaluation procedure without any fitting parameters. More sophisticated non-linear baseline descriptions have been advanced,[21, 22] however these techniques require multiple fitting parameters for the purity evaluation procedure. Near-IR absorption studies of a number of different forms of carbon, including the products of EA synthesis and commercially available carbon-based nanomaterials,[27, 28] has shown that the shape of the baseline in the range of the S_{22} interband transition depends critically on the type of nanocarbon, and this compromises the transferability of the parameters from non-linear baseline fitting procedures.

3.6.6 The NIR purity evaluation procedure implicitly assumes that the extinction coefficients of the SWNTs and carbonaceous impurities are equal on a per carbon basis. How does this affect the results of purity evaluation?

The ultimate goal of this work is the establishment of the absolute extinction coefficients which would remove this objection and allow the measurement of the absolute purity of the samples.[27, 28] The simple metric of purity adopted herein [AA(S)/AA(T)], assumes that the per carbon extinction coefficients of SWNTs and carbonaceous impurities are identical. If the extinction coefficient of the impurities is higher than that of the SWNTs, the AA(S)/AA(T) ratio would underestimate the purity, whereas the purity would be overestimated in the opposite case. Current research suggests that the extinction coefficient of SWNTs produced in the electric arc is higher than that of the carbonaceous impurities.[27, 28]

3.6.7 The NIR technique utilizes the semiconducting S_{22} interband transition for purity evaluation. What can be said about the metallic SWNTs?

The majority of known bulk synthetic techniques produce a statistical mixture of SWNTs, which corresponds to a 2:1 ratio between semiconducting and metallic SWNTs,[16] although certain CVD techniques are chirality selective.[35] Thus we assume the semiconducting S_{22} interband transition provides a measure of the purity of the whole SWNT sample.

3.6.8 Is it possible to use other solvents instead of DMF?

DMF is a good solvent for the purity evaluation technique, because it is one of the best solvents for dispersing SWNTs, does not absorb NIR radiation in the range of the S_{22} band and reduces incidental doping effect of the SWNTs. Other solvents are applicable for purity evaluation, but the AA(S)/AA(T) ratio varies among solvents. For example, we found that AA(S)/AA(T) ratio in water is lower than in DMF not only for purified (doped) material, but also for AP-SWNTs. Thus we recommend the use of a single solvent (even if not DMF) for the purity evaluation routine within a particular set of experiments.

3.6.9 Is it possible to use thin film instead of solution phase spectroscopy?

Thin film spectroscopy has been extensively used in SWNT research. Some types of SWNTs are very difficult to disperse, especially long SWNTs or purified SWNTs after high temperature annealing in vacuum. In this case some users of the NIR technique prefer to spray a thin film of SWNTs on an optical substrate for use in NIR spectroscopy. This approach is entirely legitimate,[14, 37] but we found it more difficult to obtain reproducible AA(S)/AA(T) ratios, that the results were somewhat dependent on the thickness of the film and we note that it is not trivial to obtain homogeneous non-scattering films,[29] as oppose to non-scattering dispersions.[20] Similar to the case of different solvents, the ratio AA(S)/AA(T) can be different for a sample in the solution phase and as a thin film, so it is important to be consistent in the use of either solution phase or thin film spectroscopy during a set of experiments.

3.6.10 How does debundling (rebundling) of SWNTs affect the results of the purity evaluation?

It has been shown that debundling of the SWNTs or the separation of individual SWNTs leads to better resolved absorption spectra with narrow peaks corresponding to the interband transitions of SWNTs of particular chirality.[38] Does such debundling affect the AA(S)/AA(T) ratio? To a first approximation we do not expect that debundling and the resultant change of the shape of the spectra would affect the integral values AA(S) and AA(T) and the measured purity value. However, at the present time, there are no experimental data comparing optical spectra of the same ensemble of SWNTs in individual and bundled forms, so this point remains uncertain.

3.6.11 How does the interpretation of the absorption features affect the results of the purity evaluation: Interband transitions versus Excitons

In the past few years it has been proposed, that the observed S_{11}, S_{22} and M_{11} bands do not correspond to interband transitions between pairs of Van Hove singularities, but are rather exciton bands due to the strong coupling of electrons and holes in the 1D-system.[39, 40] This issue is not finalized yet, but there are no obvious reason to suggest that a change of interpretation of the SWNT absorption feature would preclude utilization of this optical transition for purity evaluation purposes.

Acknowledgement. This work was supported by DOD/DARPA/DMEA under Awards No.DMEA90-02-2-0216 and H94003-04-2-0404.

References

1. Chen, J.; Hamon, M. A.; Hu, H.; Chen, Y.; Rao, A. M.; Eklund, P. C.; Haddon, R. C., Solution Properties of Single-Walled Carbon Nanotubes. *Science* **1998**, *282*, 95-98.
2. Kataura, H.; Kumazawa, Y.; Maniwa, Y.; Umezu, I.; Suzuki, S.; Ohtsuka, Y.; Achiba, Y., Optical Properties of Single-Wall Carbon Nanotubes. *Synth. Met.* **1999**, *103*, 2555-2558.
3. Petit, P.; Mathis, C.; Journet, C.; Bernier, P., Tuning and Monitoring the Electronic Structure of Carbon Nanotubes. *Chem. Phys. Lett.* **1999**, *305*, 370-374.
4. Chen, J.; Rao, A. M.; Lyuksyutov, S.; Itkis, M. E.; Hamon, M. A.; Hu, H.; Cohn, R. W.; Eklund, P. W.; Colbert, D. T.; Smalley, R. E.; Haddon, R. C., Dissolution of Full-Length Single-Walled Carbon Nanotubes. *J. Phys. Chem. B* **2001**, *105*, 2525-2528.
5. Hamon, M. A.; Itkis, M. E.; Niyogi, S.; Alvaraez, T.; Kuper, C.; Menon, M.; Haddon, R. C., Effect of Rehybridization on the Electronic Structure of Single-Walled Carbon Nanotubes. *J. Am. Chem. Soc.* **2001**, *123*, 11292-11293.
6. Niyogi, S.; Hamon, M. A.; Hu, H.; Zhao, B.; Bhowmik, P.; Sen, R.; Itkis, M. E.; Haddon, R. C., Chemistry of Single-Walled Carbon Nanotubes. *Acc. Chem. Res.* **2002**, *35*, 1105-1113.
7. Itkis, M. E.; Niyogi, S.; Meng, M.; Hamon, M.; Hu, H.; Haddon, R. C., Spectroscopic Study of the Fermi Level Electronic Structure of Single Walled Carbon Nanotubes. *NanoLett.* **2002**, *2*, 155-159.
8. Hennrich, F.; Lebedkin, S.; Malik, S.; Tracy, J.; Barczewski, M.; Rosner, H.; Kappes, M., Purification, Characterization and Applications of Free-Standing Single Walled Carbon Nanotube Thin Films. *Phys. Chem. Chem. Phys.* **2002**, *4*, 2273-2277.
9. Kazaoui, S.; Minami, N.; Jacquemin, R.; Kataura, H.; Achiba, Y., Amphoteric Doping of Single-Wall Carbon-Nanotube Thin Films as Probed by Optical Absoprtion Spectroscopy. *Phys. Rev. B* **1999**, *60*, 13339-13342.
10. Kazaoui, S.; Minami, N.; Matsuda, N.; Kataura, H.; Achiba, Y., Electrochemical Tuning of Electronic States in Single-Wall Carbon Nanotubes Studied by *in situ* Absorption Spectroscopy and ac Resistance. *App. Phys. Lett.* **2001**, *78*, 3433-3435.
11. Hennrich, F.; Wellmann, R.; Malik, S.; Lebedkin, S.; Kappes, M. M., Reversible Modification of the Absorption Properties of Single-Walled Carbon Nanotube Thin Films via Nitric Acid Exposure. *Phys. Chem. Chem. Phys.* **2003**, *5*, 178-183.
12. Kamaras, K.; Itkis, M. E.; Hu, H.; Zhao, B.; Haddon, R. C., Covalent Bond Formation to a Carbon Nanotube Metal. *Science* **2003**, *301*, 1501.
13. Hu, H.; Zhao, B.; Hamon, M. A.; Kamaras, K.; Itkis, M. E.; Haddon, R. C., Sidewall Functionalization of Single-Walled Carbon Nanotubes by Addition of Dichlorocarbene. *J. Am. Chem. Soc.* **2003**, *125*, 14893-14900.
14. Jost, O.; Gorbunov, A. A.; Pompe, W.; Pichler, T.; Friedlein, R.; Knupfer, M.; Reibold, M.; Bauer, H.-D.; Dunsch, L.; Golden, M. S.; Fink, J., Diameter Grouping in Bulk Samples of Single-Walled Carbon Nanotubes from Optical Absorption Spectroscopy. *App. Phys. Lett.* **1999**, *75*, 2217-2219.
15. Jost, O.; Gorbunov, A. A.; Moller, J.; Pompe, W.; Lui, X.; Georgi, P.; Dunsch, L.; Golden, M. S.; Fink, J., Rate-Limiting Processes in the Formation of Single-Wall

Carbon Nanotubes: Pointing the Way to the Nanotube Formation Mechanism. *J. Phys. Chem. B* **2002**, *106*, 2875-2883.
16. Itkis, M. E.; Perea, D.; Niyogi, S.; Love, J.; Tang, J.; Yu, A.; Kang, C.; Jung, R.; Haddon, R. C., Optimization of the Ni-Y Composition in Bulk Electric Arc Synthesis of Single-Walled Carbon Nanotubes by Using Near-Infrared Spectroscopy. *J. Phys. Chem. B* **2004**, *108*, 12770-12775.
17. Jost, O.; Gorbunov, A. A.; Liu, X.; Pompe, W.; Fink, J., Single-Walled Carbon Nanotube Diameter. *J. Nanosci. Nanotech.* **2004**, *4*, 433-440.
18. Itkis, M. E.; Perea, D.; Niyogi, S.; Rickard, S.; Hamon, M.; Hu, H.; Zhao, B.; Haddon, R. C., Purity Evaluation of As-Prepared Single-Walled Carbon Nanotube Soot by Use of Solution Phase Near-IR Spectroscopy. *Nano Lett.* **2003**, *3*, 309-314.
19. Haddon, R. C.; Sippel, J.; Rinzler, A. G.; Papadimitrakopoulos, F., Purification and Separation of Carbon Nanotubes. *MRS Bulletin* **2004**, *29*, 252-259.
20. Itkis, M. E.; Perea, D.; Jung, R.; Niyogi, S.; Haddon, R. C., Comparison of Analytical Techniques for Purity Evaluation of Single-Walled Carbon Nanotubes. *J. Am. Chem. Soc.* **2005**, *127*, 3439-3448.
21. Krestinin, A. V.; Kislov, M. B.; Ryabenko, A. G., Endofullerenes with Metal Atoms Inside as Precursors of Nuclei of Single-Walled Carbon Nanotubes. *J. Nanosci. Nanotech.* **2004**, *4*, 390-397.
22. Ryabenko, A. G.; Dorofeeva, T. V.; Zvereva, G. I., UV-VIS-NIR Spectroscopy Study of Sensitivity of Single-Wall Carbon Nanotubes to Chemical Processing and Van-der-Waals SWNT/SWNT Interaction. Verification of the SWNT Content Measurements by Absorption Spectroscopy. *Carbon* **2004**, *42*, 1523-1535.
23. Saito, R.; Fujita, M.; Dresselhaus, G.; Dresselhaus, M. S., Electronic Structure of Graphene Tubules based on C60. *Phys. Rev. B* **1992**, *46*, 1804-1811.
24. Mintmire, J. W.; Dunlap, B. I.; White, C. T., Are Fullerene Tubules Metallic? *Phys. Rev. Lett.* **1992**, *68*, 631-634.
25. Hamada, N.; Sawada, S. I.; Oshiyama, A., New One-Dimensional Conductors: Graphitic Microtubules. *Phys. Rev. Lett.* **1992**, *68*, 1579-1581.
26. Dresselhaus, M. S.; Dresselhaus, G.; Eklund, P. C., *Science of Fullerenes and Carbon Nanotubes*, Academic, San Diego, 1996.
27. Zhao, B.; Itkis, M. E.; Niyogi, S.; Hu, H.; Zhang, J.; Haddon, R. C., Study of the Extinction Coefficients of Single-Walled Carbon Nanotubes and Related Carbon Materials. *J. Phys. Chem. B* **2004**, *108*, 8136-8141.
28. Zhao, B.; Itkis, M. E.; Niyogi, S.; Hu, H.; Perea, D.; Haddon, R. C., Extinction Coefficients and Purity of Single-Walled Carbon Nanotubes. *J. Nanosci. Nanotech.* **2004**, *4*, 995-1004.
29. Lebedkin, S.; Hennrich, F.; Skipa, T.; Kappes, M., Near-Infrared Photoluminescence of Single-Walled Carbon Nanotubes Prepared by the Laser Vaporization Method. *J. Phys. Chem. B* **2003**, *107*, 1949-1956.
30. Journet, C.; Maser, W. K.; Bernier, P.; Loiseau, A.; Lamy de la Chappelle, M.; Lefrant, S.; Deniard, P.; Lee, R.; Fischer, J. E., Large Scale Production of Single-Walled Carbon Nanotubes by the Electric-Arc Technique. *Nature* **1997**, *388*, 756-758.

31. Sen, R.; Rickard, S. M.; Itkis, M. E.; Haddon, R. C., Near-IR Spectroscopy as a Tool to Monitor the Purification of Single-Walled Carbon Nanotube Films by Thermal Oxidation, in *Proceedings of the NATO Advanced Study Institute on Organic Conductors, Superconductors and Magnets: From Synthesis to Molecular Electronics*, Vol. 139 (L. Ouahab, and E. Yagubskii, Eds.), Mathematics, Physics and Chemistry, Kluwer, Corfu, Greece, 2004, pp. 143-155.
32. Hu, H.; Zhao, B.; Itkis, M. E.; Haddon, R. C., Nitric Acid Purification of Single-Walled Carbon Nanotubes. *J. Phys. Chem. B* **2003**, *107*, 13838-13842.
33. Hu, H.; Yu, A.; Kim, E.; Zhao, B.; Itkis, M. E.; Bekyarova, E.; Haddon, R. C., Influence of the Zeta Potential on the Dispersability and Purification of Single-Walled Carbon Nanotubes. *J. Phys. Chem. B* **2005**, *109*, 11520-11524.
34. Kim, Y.; Luzzi, D. E., Purification of Pulsed Laser Synthesized Single Wall Carbon Nanotubes by Magnetic Filtration. *J. Phys. Chem. B* **2005**, *ASAP*.
35. Resasco, D. E.; Herrera, J. E.; Balzano, L., Decomposition of Carbon-Containing Compounds on Solid Catalysts for Single-Walled Nanotube Production. *J. Nanosci. Nanotech.* **2004**, *4*, 398-407.
36. Zheng, M.; Jagota, A.; Strano, M. S.; Santos, A. P.; Barone, P.; Chou, S. G.; Diner, B. A.; Dresselhaus, M. S.; Mclean, R. S.; Onoa, G. B.; Samsonidze, G. G.; Semke, E. D.; Usrey, M. L.; Walls, D. J., Structure-Based Carbon Nanotube Sorting by Sequence-Dependent DNA Assembly. *Science* **2003**, *302*, 1545-1548.
37. Sen, R.; Rickard, S. M.; Itkis, M. E.; Haddon, R. C., Controlled Purification of Single-Walled Carbon Nanotube Films by Use of Selective Oxidation and Near-IR Spectroscopy. *Chem. Mater.* **2003**, *15*, 4273-4279.
38. O'Connell, M. J.; Bachilo, S. M.; Huffman, C. B.; Moore, V. C.; Strano, M. S.; Haroz, E. H.; Rialon, K. L.; Boul, P. J.; Noon, W. H.; Kittrell, C.; Ma, J.; Hauge, R. H.; Weisman, R. B.; Smalley, R. E., Band Gap Fluorescence from Individual Single-Walled Carbon Nanotubes. *Science* **2002**, *297*, 593-596.
39. Ando, T., Excitons in Carbon Nanotubes. *J. Phys. Soc. Japan* **1997**, *66*, 1066-1073.
40. Spataru, C. D.; Ismail-Beigi, S.; Benedict, L. X.; Louie, S. G., Excitonic Effects and Optical Spectra of Single-Walled Carbon Nanotubes. *Phys. Rev. Lett.* **2004**, *92*, 077402-1 - 077402-4.